

# A Quantitative Measure of the Richness of Galaxy Clusters

H. K. C. Yee<sup>1,2</sup>, and Omar López-Cruz<sup>1,2,3</sup>

## ABSTRACT

Using photometric catalogs from wide-field CCD images, we derive the cluster-galaxy correlation amplitudes,  $B_{gc}$ , for 47 low-redshift Abell clusters. We apply a number of tests to establish the robustness of the  $B_{gc}$  parameter as a quantitative measure of richness of galaxy clusters. These include using different galaxy luminosity functions to normalize the excess galaxy counts, counting galaxies to different absolute magnitude limits, and counting galaxies to different cluster-centric radii. These tests show that with a properly normalized luminosity function, the  $B_{gc}$  parameter is relatively insensitive (at better than 1/2 of an Abell Richness class) to magnitude limit, areal coverage, and photometric errors of up to about 0.25 mag. We compare the  $B_{gc}$  values to both the Abell Richness Class (ARC) and Abell count numbers ( $N_A$ ). It is found that there is a good correlation between  $B_{gc}$  and  $N_A$  for Abell clusters with  $z \lesssim 0.1$ , with a dispersion of about one ARC; whereas the Abell Richness classifications for Abell clusters at  $z \gtrsim 0.1$  are much less well correlated with the true cluster richness. We also find evidence that the richness of  $\text{ARC} \geq 3$  clusters has the tendency of being over estimated in the Abell catalog.

*To appear in The Astronomical Journal, May 1999*

## 1. Introduction

The richness is an important defining attribute of a galaxy cluster, yet has always proven to be difficult to quantify rigorously. Abell (1958), in creating the first comprehensive catalog of rich galaxy clusters, defined the richness classification which now bears his name based on the number of galaxies within 2 mag of the third ranking galaxy in an angular area of radius  $1.7'/z$ , or about 3 Mpc (for  $H_0 = 50 \text{ km s}^{-1} \text{ Mpc}^{-1}$ ). The procedure that Abell used in counting the number of galaxies from Palomar Sky Survey Prints must be considered approximate, and difficult

---

<sup>1</sup>Department of Astronomy, University of Toronto, Toronto, Ontario M5S 3H8, Canada, Email: hyee@astro.utoronto.ca

<sup>2</sup>Visiting Astronomer, Kitt Peak National Observatory, KPNO is operated by AURA, Inc. under contract to the National Science Foundation.

<sup>3</sup>Instituto Nacional de Astrofísica, Óptica y Electrónica (INAOE), Tonantzintla, Pue., México, Email: omar@inaoe.mx

to extend to higher redshift. The accuracy of the Abell classification for Abell clusters is accurate probably to only about 1 class (e.g., see Dressler 1978). Uncertainties can arise from many sources: inaccurate estimate of photometry, poor star-galaxy classification, incorrect background correction, contamination from foreground or background clusters, and large uncertainty in the estimated redshift. In addition, the relatively large area used for the counting increases the chance of contaminating projections. At higher redshift, most of these problems would only be magnified, making a similar richness classification impractical without additional data such as accurate photometry and redshift. Furthermore, at redshifts higher than  $\sim 0.2$ , it becomes increasingly more difficult, if not impossible, to specify, for example, the third brightest cluster member, due to the large number of foreground galaxies.

A robust richness measurement for galaxy clusters is an important observational quantity. Beside being one of the primary attributes of a cluster, it can be used as a baseline for comparing other properties of clusters in a meaningful way. This is especially important as advances in technology have allowed us to study galaxy clusters at different epochs and at increasingly higher redshifts, up to and above 1 (e.g., Dickinson 1997). Ultimately, a more fundamental parameter is the mass of the cluster. However, there is evidence that the richness of a cluster, properly determined, can be a good predictor of the mass of the cluster (Carlberg et al. 1996, and Yee et al. 1999) based on results from the CNOC1 cluster redshift survey.

Various attempts have been carried out to produce a more accurate measure of the richness of Abell clusters. These include the  $N_{0.5}$  of Bahcall (1981), and the revised Abell Count Numbers,  $N_A$ , of Abell, Corwin, & Olowin (1989, hereafter ACO). To arrive at a robust and rigorous quantitative measure of cluster richness, three observational issues must be taken into account when counting the number of galaxies in a cluster: the angular coverage, the depth of the observation, and the background correction. The availability of wide field digital imaging due to advances in large format CCDs has enabled us to address these issues quantitatively much better. The wide field allows us to sample the bulk of even very low redshift clusters, and digital imaging provides us with accurate photometry, which is vital for determining the depth of the galaxy counts, and correcting for background. In addition, a useful quantitative richness measure is one that can be applied uniformly to different samples at vastly different redshifts.

The cluster-center galaxy correlation amplitude ( $B_{gc}$ ), first used by Longair & Seldner (1979) to quantify the environment of radio galaxies, is one parameter that appears to be well-suited as a robust richness parameter. By assuming an universal luminosity function (LF) and spatial profile, the excess galaxy counts around any reference point can be properly corrected to create an unbiased estimator of the richness of the environment. Yee & Green (1987) extended the method to study the environment of quasars by using a “universal” LF with evolution that is self-consistent with the background galaxy counts. The ability to track the evolution of the LF at different epochs is extremely important in comparing richness of clusters at different redshifts in a meaningful way. However, although such a method has been used in many studies of the environments of active objects, fully digital photometric data have not been applied to the quantification and calibration

of the richness of ordinary galaxy clusters, such as the Abell clusters, and to test the robustness of the parameter.

In this paper, we present the richness measurements, in the form of  $B_{gc}$ , for a sample of 47 Abell clusters based on digital photometric data. These measurements can be used as a calibration between the  $B_{gc}$  parameter and the more traditional Abell richness class (hereafter, ARC). We show that  $B_{gc}$  is a robust richness estimator, provided that a galaxy LF well matched to that found in clusters is used for normalization. We find that there is a good correlation between the  $N_A$  and  $B_{gc}$  for clusters at  $z \lesssim 0.1$  with a dispersion of about 1 richness class. However,  $z > 0.1$ ,  $N_A$  often over-estimates the true richness of Abell clusters.

In §2 we present the sample and the data set. The method for deriving  $B_{gc}$  is briefly discussed in §3, along with the LFs used in the computation. In §4 we test the robustness of the  $B_{gc}$  parameter by investigating the dependence of the parameter on various quantities such as the LF, magnitude limit, and sampling area. Section 5 discusses the results and compare the ARC with the  $B_{gc}$  parameter. A summary is presented in §6. Throughout this paper, unless otherwise specified, we use  $H_0 = 50 \text{ km s}^{-1} \text{ Mpc}^{-1}$  and  $q_0 = 0.1$ .

## 2. The Cluster Sample and Data

The data used in this work are from a sample of Abell clusters originally chosen for a study of correlations between X-ray and optical properties (the Low-Redshift Cluster Optical Survey (LOCOS), see López-Cruz & Yee 1999). The detailed description of the sample, observation, and data reduction can be found in López-Cruz (1997, hereafter LC97). Here, we present a brief summary.

The clusters were selected from a compilation of bright X-ray clusters made by Jones & Foreman (1998) with the following criteria: (1) galactic latitude  $|b| \geq 30^\circ$ ; (2)  $0.04 < z < 0.20$ ; (3)  $\text{ARC} \geq 1$ ; and (4) the declination  $\delta \geq 24^\circ$ . Although there is an imposed criterion of  $\text{ARC} \geq 1$ , data for a number of  $\text{ARC}=0$  clusters were also obtained, often for the purpose of filling Right Ascension gaps during the observing runs. The  $\text{ARC}=0$  clusters are not considered as part of the fair sample. This is because they were not picked randomly; ones that appear to be rich or have well-defined X-ray emission were preferentially chosen. Nevertheless, they are analysed along with the other clusters, but are used only when such a selection effect does not affect the particular conclusion. As a comparison, the central region of Coma (A1656,  $z = 0.0232$ ) was also observed. The total number of Abell clusters in the sample is 47, with 36 satisfying the criteria listed above. The cluster names, along with their redshifts and Abell Richness Classes, are listed in Table 1.

Direct images in  $B$ ,  $R$ , and  $I$  were obtained using the T2KA CCD camera at the 0.9m telescope at KPNO over five runs in 1992 and 1993. Photometry was calibrated to the Johnson-Kron-Cousin system of Landolt (1992). The CCD has  $2048 \times 2048$  pixels with a scale of  $0.68'' \text{ pixel}^{-1}$ , giving a field of view of  $23.2' \times 23.2'$ . The integration times varied between 900 to 2500 second, depending

on the filter used and the redshift of the cluster.

Nine control fields at least  $5^\circ$  away from any cluster fields were also observed for the purpose of background count correction. These fields were observed and reduced in an identical manner as the cluster fields.

Photometric catalogs of all objects in each field were created using the program PPP (Yee 1991) to perform automatic object finding, photometry, and galaxy-star classification. The typical 100% completeness magnitude in  $R$  is  $\sim 21.5$  mag. This provides a range of completeness in absolute  $R$  magnitudes at the redshift of the clusters from  $-15.5$  to  $-18.5$ .

### 3. Analysis

#### 3.1. The $B_{gc}$ Parameter

The cluster richness parameter  $B_{gc}$  is defined as the amplitude of the cluster center–galaxy correlation function:

$$\xi(r) = B_{gc} r^{-\gamma}. \quad (1)$$

This parameter was first used by Longair & Seldner (1979) to quantify the richness of radio galaxy environment. It was subsequently adopted by Yee & Green (1984) to study the environment of quasars using a self-consistent LF estimated from the same data. Further applications of the parameter to the study of the environments of quasars and radio galaxies can be found in Yee & Green (1987; hereafter YG87); Ellingson, Yee, & Green (1991); Prestage & Peacock (1988); and Yates, Miller, & Peacock (1989). This method has also been used to quantify the environment of BL Lacertae objects (Smith, O’Dea, & Baum 1995; Wurtz et al. 1997), Seyfert galaxies (De Robertis, Yee, & Hayhoe 1998), and the richness of a small sample of Abell clusters (Anderson & Owen 1994). Detailed descriptions of the method adopted for this study can be found in YG87, and also Andersen & Owen (1994), among others. Here, we provide a brief outline.

We observe galaxies in projection on the sky, which allows us to measure the angular two-point correlation function of galaxies,  $\omega(\theta)$ , as a function of the angle  $\theta$  on the sky. The function  $\omega(\theta)$  can be approximated by a power-law of the form (e.g., Davis & Peebles 1983):

$$\omega(\theta) = A_{gg} \theta^{1-\gamma}. \quad (2)$$

where  $A_{gg}$  is the galaxy-galaxy angular correlation amplitude. For our purpose, we can interpret  $\omega(\theta)$  as the distribution of galaxies projected on the sky around a reference point, such as the center of a galaxy cluster. In this case, the amplitude, now notated as  $A_{gc}$ , can be measured directly from an image by counting the excess (i.e., background corrected) galaxy counts,  $N_{net}$ ,

up to a certain apparent magnitude around this reference point within some  $\theta$ ; i.e., if a fixed  $\gamma$  is assumed, then  $A_{gc} = \frac{N_{net}}{N_{bg}} \frac{(3-\gamma)}{2} \theta^{\gamma-1}$ , where  $N_{bg}$  is the background counts within  $\theta$ .

The  $B_{gc}$  amplitude can then be estimated via a deprojection of the angular correlation function into the spatial correlation function by assuming spherical symmetry, giving the relation between  $B_{gc}$  and  $A_{gc}$  (see Longair & Seldner 1979):

$$B_{gc} = N_{bg} \frac{D^{\gamma-3} A_{gc}}{I_{\gamma} \Psi[M(m_0, z)]}, \quad (3)$$

where  $N_{bg}$  is the background galaxy counts to apparent magnitude  $m_0$ ;  $\Psi[M(m_0, z)]$  is the integrated LF of galaxies up to the absolute magnitude  $M$  corresponding to  $m_0$  at the redshift of the cluster  $z$ .  $I_{\gamma}$  is an integration constant arising from the deprojection, (with  $I_{\gamma} = 3.78$  for  $\gamma = 1.77$ ), and  $D = \frac{c}{H_0} \{q_0 z + (q_0 - 1)[(2q_0 z + 1)^{\frac{1}{2}} - 1]/q_0^2(1+z)^2\}$  is the angular diameter distance to  $z$ .

As eqn (3) indicates, the computation of  $B_{gc}$  requires a knowledge of the luminosity function (which provides a normalization) and a background count correction. These are described in the next two subsections.

### 3.2. The Control Field Counts

The background counts used were obtained from the same cluster imaging program using the same telescope-CCD-filter combination and the same reduction procedure, which are described in detail in LC97. Briefly, 9 fields with integration times similar to those of the cluster fields were obtained at least  $5^\circ$  from any of the program clusters. The control field counts were combined using the technique described in Yee, Green, & Stockman (1986). Figure 1 shows the counts. These counts are in good agreement with the red band counts from other investigations (e.g., Driver et al. 1994, Metcalfe et al. 1991, and Yee et al. 1986). Using background counts obtained in an identical manner as the cluster data removes one of the major systematic uncertainties in the determination of  $B_{gc}$ .

### 3.3. The Luminosity Function

The choice of the LF used is a crucial one in the determination of  $B_{gc}$ . The sensitivity of the  $B_{gc}$  value to the LF will be discussed in detail in §4.1. The assumption of a universal LF is not strictly correct, as field and cluster galaxies have different population mixes and evolution histories. However, for the computation of  $B_{gc}$  using galaxies brighter than  $\sim -18$  mag, the varying faint-end slope of cluster galaxy LF (López-Cruz et al. 1997) has little or no effect. We choose to test three LFs derived from very different data sources and methods. They are all

represented functionally by the Schechter function (Schechter 1976). The three functions are (1) the LF derived from the clusters themselves (López-Cruz & Yee 1999, hereafter the LCY LF); (2) the low-redshift field galaxy LF from King & Ellis (1985, hereafter the KE LF); and (3) the field galaxy LF from the CNOC2 redshift survey of intermediate redshift galaxies (Lin et al. 1999, hereafter the CNOC2 LF). The parameters of the LFs are listed in Table 2 and the LFs are described in the following. We will first discuss primarily the shape of the LFs used and defer the description of the normalization of the LFs to later in the section.

We derive the shape of the LCY LF using the cluster data themselves. The derivation of the LF for this sample of clusters is described in detail in LC97, López-Cruz et al. (1997), and López-Cruz & Yee (1999). The bright end is fitted to a Schechter function with  $\alpha = -1.0$ . The result (LC97, López-Cruz & Yee 1999) shows that the sample has  $\langle M^* \rangle = -22.26 \pm 0.29$ , where the uncertainty is the dispersion of the distribution. However, cD clusters appear to have a larger range of  $M^*$  which is apparently correlated with richness (LC97, López-Cruz & Yee 1999). Removing the cD clusters produces a  $\langle M^* \rangle = -22.32 \pm 0.26$ . We adopt an “universal” LF for the clusters with  $M^* = -22.3$  (at a median redshift of 0.07) and  $\alpha = -1.0$ .

For deriving richness measurements for clusters at significant redshifts, the evolution of galaxies comes into play. Counting galaxies to a fixed absolute magnitude will in general overestimate the richness for high redshift clusters, as even mild passive evolution will mean effectively counting deeper into the LF. Hence, following YG87, we add a mild luminosity evolutionary term parametrized as  $-Qz$  mag, where  $Q \sim 1.4$ , to  $M^*$  to compensate for this effect. (YG87 used a second order polynomial for  $M^*$  evolution, we have simplified this to a single term in  $z$ , since any such measurement is currently extremely approximate.) There is good evidence that the LF in clusters evolves, to first order, in such a manner from galaxies associated with quasars (YG87), and from the CNOC1 cluster redshift survey (Yee et al. 1999). Since the median redshift for the LC97 clusters is 0.07, we correct the  $M^*$  to redshift 0 to  $\sim -22.2$ .

For a consistency check with previous applications of the  $B$  parameters in analyses of the environments of quasars (e.g., YG97), radio galaxies (Yates et al. 1989), BL Lacs (Wurtz et al. 1997), and Seyfert galaxies (De Robertis et al. 1998), we also compare  $B_{gc}$  values using the field galaxy KE LF with its separate components for different morphological types. The KE LF was derived as a preliminary result using a small number of low-redshift galaxies from the AAT/Durham redshift survey. Here, the  $M^*$  values are transformed into the Cousin  $R$  band from the Gunn  $r$  band as listed in YG87. The same luminosity evolution as that for the LCY LF is incorporated into the KE LF.

The final LF used is the interim LF derived from the CNOC2 field galaxy redshift survey (Yee et al. 1997, Lin et al. 1999). The LF is determined based on about 2300 galaxies with redshifts between 0.1 and 0.55, covering two patches on the sky. The galaxies are separated into early, intermediate, and late spectral types based on 5-color photometry. The LF for each component is then fitted to a Schechter function with two evolution parameters,  $P$  and  $Q$ , in the form of

$\Phi(z, M) = \Phi(0, M - Qz)10^{0.4Pz}$  (see Lin et al. 1999 for details). Hence, the evolution of this LF is derived explicitly with  $Q$  measuring the luminosity evolution, and  $P$ , the density evolution (see Table 2).

An important parameter in the LF for the determination of  $B_{gc}$  is the normalization constant  $\phi^*$ . The value of  $B_{gc}$  is inversely proportional to it. As discussed in YG87, the best way to minimize systematic effects in  $B_{gc}$  is to determine a self-consistent LF with a normalization constant that reproduces the background counts as a function of apparent magnitude. We hence renormalized  $\phi^*$  by multiplying it by  $\phi'$  which is determined by fitting the modeled counts to the background counts. We determine  $\phi^*$  for the LCY LF directly by minimizing the  $\chi^2$  between model counts generated by using the LF and the background count data. For the KE and CNOC2 LFs, the relative  $\phi^*$ 's for each component are retained, but an overall normalization is applied based on the background count fitting. We found that the renormalization of the CNOC2 LF, which is derived using the same photometry band, is small, less than 10%. The modeled counts for the various LFs are shown in Figure 1.

### 3.4. Results and Error Estimate

The  $B_{gc}$  values obtained using the LCY LF are listed in Table 1. The values obtained using the other two LFs are similar, with variations of less than  $\sim 10\%$ . A more detailed comparison of the dependence of  $B_{gc}$  on the LF is left to Section 4.1. For each cluster, we count galaxies down to a limit of  $M_R = -20$  in a circle of 0.5 Mpc radius nominally using the brightest cluster galaxy (BCG) as the center of the cluster. However, we note that a few clusters have their BCG not sitting in the obvious center of the distribution of galaxies. The most significant deviation occurs in A168, where the BCG is almost isolated from the cluster. In this case, we have chosen the brightest galaxy in the high density clump (with the correct color) to be the center of the cluster. Choosing the BCG as the center for A168 would produce a  $B_{gc}$  almost 3 times smaller.

The uncertainty for the  $B_{gc}$  parameter is computed using the formula:

$$\frac{\Delta B_{gc}}{B_{gc}} = \frac{(N_{net} + 1.3^2 N_{bg})^{1/2}}{N_{net}}. \quad (4)$$

where  $N_{net}$  is the net counts of galaxies over the background of  $N_{bg}$ . This is a conservatively large error estimate as it includes the expected counting statistics in  $N_{net}$  and the expected dispersion in background counts. The factor  $1.3^2$  is included to account approximately for the additional fluctuation from the clustered (and hence non-Poissonian) nature of the background counts (see LC97 and YG87). This is a fair estimate of the uncertainty of the richness of the cluster, as it includes the Poissonian uncertainty in the net counts, which is equivalent to the uncertainty in the number of galaxies drawn from a Schechter function with a fixed normalization (hence of fixed richness). However, we note that the inverse of this error estimate is an underestimate

of the statistical significance of the excess galaxy counts in the sample, which would be better represented by  $N_{net}/1.3(N_{bg})^{1/2}$ . Hence, at these low redshifts, while the average uncertainty in the  $B_{gc}$  parameter is about 25%, the significance of the excess counts over background is considerably better at about the  $20\sigma$  level.

#### 4. The Robustness of the $B_{gc}$ Parameter

In this section, we examine the results of exhaustive tests on the dependence of  $B_{gc}$  on various quantities, such as the LF shape and parameters, sampling and spatial limits, and photometric errors. These tests not only provide a clear indication of the robustness of the  $B_{gc}$  parameter, but also the pitfalls in applying the method.

##### 4.1. The Dependence of $B_{gc}$ on the Luminosity Function

A richness measurement based on the number of galaxies in a cluster is invariably tied to the assumption of the luminosity function of the galaxies. If clusters have greatly different galaxy LFs, then any such richness measurement would be rendered meaningless. In this section, we test the sensitivity of  $B_{gc}$  to the LF used in converting  $A_{gc}$  to  $B_{gc}$ . For these tests we vary the LF parameters but fix the sampling limit at  $M_R = -20$  mag. This sampling limit was chosen with the expectation that it minimizes the effect of having an incorrect LF. Varying the LF with different sampling limits causes more complex behaviors; these effects are tested in §4.2.

###### 4.1.1. Comparing Results from Different Luminosity Functions

We have computed  $B_{gc}$  using three LFs derived using very different data and method. The LCY LF is based on the cluster LF measured from the same set of data, and describes cluster galaxies the best; while the KE and CNOC2 LF are based on field galaxies at different redshifts. The three give remarkably similar results with the mean of the ratio of  $B_{gc}(\text{LCY}):B_{gc}(\text{CNOC2}):B_{gc}(\text{KE})$  being 1.00:1.10:0.92, with the mean value for  $B_{gc}(\text{LCY})$  being  $1246 \pm 417$ , where the uncertainty is the dispersion of the  $B_{gc}$  values in the sample. This result demonstrates that the systematic uncertainty arising from the not-strictly-correct assumption of a “universal” LF for both cluster and field galaxies is of the order of 10%. The ratios indicate that the CNOC2 LF is slightly fainter overall compared to the LCY LF, while the KE LF is somewhat brighter. This indeed is the case when comparing the  $M^*$ ’s of early type galaxies in the two multi-component LFs with that of the LCY LF.

For the remainder of the paper, we will use the  $B_{gc}$  values derived using the LCY LF as the fiducial set, and compare the results from the various tests to it.



#### 4.1.2. *The Effect of an Incorrect Luminosity Function*

First, we test the effect of an “universal” LF with incorrect parameters. In varying the  $M^*$  and  $\alpha$  of the LF, we also adjust the normalization constant of the LF, so that it reproduces the control field galaxy counts up to the magnitude of sampling. Note that this is an important step to make sure that the  $B_{gc}$ ’s are obtained with a self-consistent LF model. This is different from testing the effects of statistical fluctuations of the LF of individual clusters from the mean for which one would not perform the renormalization (see §4.1.3).

In these tests we first adjust the LCY LF by altering  $M^*$  in steps of  $\pm 0.25$  mag. Each time we recompute the normalization constant for the LF by fitting the background counts. We note that the fit to the background counts deteriorates with each step, but remains reasonable up to a  $\Delta M$  of  $\pm 0.5$  mag. The results are summarized in Table 3. The results for  $M^*$  being off by  $\pm 0.25$  mag are quite acceptable, causing variations of about 10%, similar to the effects of using the three different LFs. This is not surprising, as the uncertainties in the three LFs are of the same order. Even when the error is 0.5 mag, the effect is about 20%, comparable to about 1/2 an Abell Richness Class (equivalent to  $\Delta B_{gc}$  of about 200; see Section 5).

We next alter the faint-end slope  $\alpha$  of the LF, again, with renormalization based on fitting the background. Here, we change  $\alpha$  by steps of 0.15. The results are tabulated in Table 4. Again, one sees that changing the slope by as much as  $\pm 0.3$  alters the  $B_{gc}$  values by less than 20%.

These tests, along with the results from using three different LFs, demonstrate that a LF which self-consistently reproduces the background counts can be substantially incorrect and still produces results that are accurate to better than 1/2 an Abell class.

#### 4.1.3. *The Effect of Fluctuations in the Cluster Galaxy Luminosity Function*

In this section, we test the effect of statistical fluctuations from the mean in the LF of the cluster galaxies. Here, we vary  $M^*$  and  $\alpha$ , but do not adjust the normalization constant of the LF. Note that in the case of  $M^*$ , it has the same effect as a photometric error of the same magnitude in the cluster data.

We use the same step sizes for  $M$  and  $\alpha$  as in §4.1.2, and the results are listed in Tables 3 and 4. Here, we see that the effects are significantly larger. Specifically, a fluctuation in  $M^*$  (or equivalently, photometric error in the data) of about 0.4 mag will produce a 20% (1/2 Abell class) effect. However, a fluctuation of 0.2 mag would still be quite acceptable, producing uncertainties of only about 10%. Since cluster  $M^*$ ’s have a dispersion of about 0.2 mag, this indicates that the intrinsic dispersion of the LF from cluster to cluster does not affect  $B_{gc}$  significantly. Similar fluctuations due to variations in  $\alpha$  of up to 0.3 are also seen.

#### 4.2. The Dependence of $B_{gc}$ on the Limiting Magnitude

The independence of  $B_{gc}$  values on galaxy counting limiting magnitude is an important issue, especially when different fields are observed to different depths. If the correct LF is chosen for the computation of  $B_{gc}$  and the LF is truly universal, then  $B_{gc}$  should subject only to counting statistical variations when different limiting magnitudes are used. A substantial systematic variation in  $B_{gc}$  with limiting magnitude can be taken as an indication that a LF with the incorrect shape has been chosen. Moreover, for the purpose of producing robust results, there is an optimal range of absolute magnitudes for galaxy counting. Counting to too bright a limit will produce a large uncertainty from counting statistics. Furthermore, one is at the mercy of small intrinsic variations of  $M^*$  in individual clusters, or equivalently, small photometric zero point error in the galaxy photometry.

On the other hand, a larger uncertainty may also result from counting too deep into the LF, as the background counts rise more rapidly than the flat part of the cluster LF. In addition, in counting beyond  $M_R \sim -18$  one may encounter large variations in the faint end slopes of the cluster LF (López-Cruz et al. 1997 and LCY), producing additional fluctuations. Ideally, one would like the richness parameter of a galaxy cluster to be representative of the total mass of the cluster, which, under the light-traces-mass scenario (e.g., Tyson & Fischer 1996; Carlberg, Yee, & Ellingson 1997), should be proportional to the total light. Hence, the richness of a cluster is best represented by the number of  $L^*$ -like galaxies, rather than by the number of dwarf galaxies; consequently, a robust measure of  $B_{gc}$  is best obtained using a magnitude limit corresponding to the flat part of the LF: from about 1 mag to 3 mag past  $M^*$ .

The data in our sample of Abell clusters sample to at least  $M_R = -18.5$  mag for all the clusters; hence, they provide a good test on the robustness of  $B_{gc}$  versus counting magnitude, and the effects of varying the LF. For these tests, we compute the  $B_{gc}$  parameters using  $M_R = -22.0, -21.0, -20.0, -19.0$ , and  $-18.0$  for comparison with the standard limit of  $-20$  (i.e., about 2 mag past  $M^*$ ). The five derivations provide ratios of average  $B_{gc}$  of: 1.04:1.05:1.00:1.00:1.07. A comparison of the individual  $B_{gc}$ 's using sampling limits of  $-21.0$  and  $-20.00$  is shown in Figure 2. This test shows very strongly that, as expected, when a LF closely resembling that of the cluster galaxy LF is used, the sampling magnitude limit has little or no systematic effect on the derived richness. The variations in individual  $B_{gc}$  values are the order of the computed uncertainties, and are due to counting statistics. We note that the largest deviation occurs with the deepest sampling limit. This is expected as the steepening of the galaxy LF for some clusters begins at about  $M_R = -18$ , which would produce a larger count relative to the flat ( $\alpha = 1$ ) LF used.

Next, we consider the effects of the combination of LF variations and more extreme sampling limits. We focus on testing the effect of incorrect LF and photometric errors when sampling to only about  $M^*$ , a situation that may arise often when data which are not quite deep enough are pressed into use. The results are shown in Table 3. In general, at a sampling limit of  $M_R = -22$  mag (about  $M^*$ ), the errors committed when  $M^*$  is varied with renormalization of the LF (equivalent

to using an incorrect LF) are about twice as large as those when the sampling is to  $\sim 2$  mag past  $M^*$  (about  $-20$  mag). However, when no renormalization is performed, which is also equivalent to photometric uncertainty, the errors incurred when counting to  $-22$  mag can be as large as 4 times those to  $-20$  mag. For example, a  $+0.5$  mag change in  $M^*$  produces  $B_{gc}$  values 2.2 times larger when counting to  $-22$  mag, compared to 1.3 times larger when counting is done to  $-20$  mag. We note that the results for changing  $\alpha$  are not nearly as drastic, as that affects mainly the faint end of the LF (see Table 4).

We hence conclude that counting to about  $M^*$  produces results that are extremely sensitive to errors in the assumed LF, photometry, and in general statistical fluctuation, with results that could be off by a factor of 1.5 to over 2 when the error in magnitude is 0.25 to 0.5 mag. This may explain the large discrepancies noted in the  $B_{gc}$  values of BL Lac objects between Smith, O’Dea, & Baum (1995) and Wurtz et al. (1997), as noted by Wurtz et al.. We also note that this may also be the possible explanation of the discrepancies of between the richness derived for Abell clusters by Andersen & Owen (1994) and this work (see §5.1).

### 4.3. The Dependence of $B_{gc}$ on Sampling Area

Ideally, a robust richness parameter is one such that the counting area used should not have a significant effect on the richness derived. Such a parameter would allow comparison of the richness parameter from data taken with a wide variety of areal coverage. This is strictly possible only if the spatial distribution function of cluster galaxies has a similar form for all clusters. If an incorrect slope ( $\gamma$ ) for the correlation function is used, the  $B_{gc}$  value will be dependent on the sampling area. In the computation of  $B_{gc}$  it is assumed that the galaxy distribution drops off in the same fashion as the spatial correlation function for field galaxies. This assumption is adopted so that comparisons over a wide range of richness and environments, including that of field galaxies, can be made. However, this assumption is most likely incorrect for rich clusters, as various investigations have shown that the power-law slope of their galaxy density distribution is probably greater than 2 (e.g., Lilje & Efstathiou 1988, Peebles 1993), somewhat steeper than that of the clustering of field galaxies.

The effect of using an inexact  $\gamma$  can be examined by comparing the  $B_{gc}$  values for our sample using different limiting radii. We have computed  $B_{gc}$  values (with the LCY LF) using sampling radii of 0.25, 0.5, 1.0 Mpc, all with a  $M_R$  sampling limit of  $-20$  mag. The ratio of the mean  $B_{gc}$ ’s for the 3 radii are: 1.03:1.00:0.94. The results for individual clusters with sampling radii of 0.5 and 1.0 Mpc are shown in Figure 3.

The results indicate that a change of a factor of 2 in the sampling radius causes a scattering of about 5% in the richness parameter. This small effect is reassuring, and provides confidence when comparing data sampled over metric field sizes of a factor of several, as in those used by De Robertis et al. (1998) for nearby Seyfert galaxies. The decreasing trend in the  $B_{gc}$  with larger

radii is consistent with existing evidence that cluster galaxy distribution is likely to be steeper than the slope of the field galaxy correlation function. However, since the effect is very small, we have chosen to retain the canonical  $\gamma = 1.8$  so that direct comparisons with field and group clustering amplitudes can be made.

## 5. Discussion

The various tests in Section 4 have established the robustness of the  $B_{gc}$  parameter as a measure of cluster richness. In this section, we compare the  $B_{gc}$  parameter with the Abell Richness Class, establishing a calibration between the two. We also discuss the correlation between  $B_{gc}$  and the Abell count number, which allows us to examine the accuracy of the Abell count number as a measure of richness. Based on these comparisons, we suggest a revised richness classification scheme based on the calibration between the  $B_{gc}$  parameter and ARC. Finally, we illustrate the advantage of using a robust richness parameter in the investigation of cluster properties by examining the correlation between richness and velocity dispersion.

### 5.1. Comparison with Abell Richness Class

One of the main goal of this investigation is to establish a calibration between a more quantitative richness parameter, such as  $B_{gc}$ , and the traditional Abell Richness Class. In Figure 4, we plot the  $B_{gc}$  parameters versus ARC. We see in general a very broad correlation between  $B_{gc}$  and ARC. We note that because we have specifically chosen to image ARC 0 clusters which appear to be the richest, they should not be considered in the correlation.

Andersen & Owen (1994) produced a qualitatively very similar plot of the two quantities using a different sample and very different type of data. However, quantitatively, there is a significant discrepancy in the scaling of the two quantities: Their  $B_{gc}$  values are close to a factor of two lower than ours (after correcting for  $H_0$ ), with their average  $B_{gc}$  for ARC 1 clusters being  $\sim 600 \text{ Mpc}^{-1.8}$ , compared to about  $1000 \text{ Mpc}^{-1.8}$  in our work. This discrepancy is perhaps not surprising, given that: (1) Andersen & Owen use POSS photographic data which may not be well calibrated, (2) their object counting goes down to only  $\sim M^*$ , and (3) they did not use a LF that has been renormalized to the background. All these can contribute substantially to the systematic uncertainty, up to a factor of 2, as demonstrated by our tests in §4.

Since the ARC is an approximate and quantized measure, we will next look at the comparison with actual Abell counts ( $N_A$ ) before revisiting the correlation between  $B_{gc}$  and ARC in §5.3.

## 5.2. Comparison with Abell Count Numbers

A more detailed comparison between the ARC and the  $B_{gc}$  measurement can be obtained by using the Abell number counts ( $N_A$ ) as published by ACO. We plot  $N_A$  vs  $B_{gc}$  in Figure 5. Taken as a whole, again we see a definite correlation between  $B_{gc}$  and  $N_A$  but with a large dispersion. Specifically, it is noted that at large  $N_A$  the correlation breaks down in that their corresponding  $B_{gc}$  values are smaller than indicated by  $N_A$ . We also note that all the clusters in our sample with large  $N_A$ s are those at higher redshifts. We hence break the sample into two groups, dividing them at  $z = 0.09$ . To increase the  $z > 0.09$  sample, we also add 3 clusters from the CNOC1 survey (Yee et al. 1999) which are Abell clusters at  $z \sim 0.2$ . These are A2390, MS0451+02 (A520), and MS0906+11 (A750).

Removing the high redshift sample provides a much improved correlation between  $B_{gc}$  and  $N_A$ . For the lower  $z$  sample, though the scatter is about one Abell class, there are few or no outliers. For the higher  $z$  sample, there is almost no correlation between  $B_{gc}$  and  $N_A$ . The discrepancies come entirely in the high  $N_A$  clusters which all have too large a  $N_A$  for their  $B_{gc}$ . It is interesting to note that A665, which is the only Abell cluster classified as ARC 5, with  $N_A = 321$ , has a  $B_{gc}$  value which indicates that its richness is overestimated by a factor of 3 by  $N_A$ . A number of Abell clusters in fact have similar richness to A665, including A2390 and A401. Hence, we conclude that at  $z \lesssim 0.1$ , the ACO counts provide reasonable estimates of the richness of the clusters; however, at  $z \gtrsim 0.1$ , and/or for  $N_A \gtrsim 140$ , the  $N_A$  counts almost always over predict the cluster’s richness. This is not a surprising result, as many authors have concluded that the Abell catalog becomes incomplete at  $z \gtrsim 0.1$  (e.g., Southerland 1988; Struble & Rood 1991b).

## 5.3. A $B_{gc}$ Calibrated Richness Classification

Using Figures 4 or 5, we can relate the more robust  $B_{gc}$  measurements directly to the Abell Richness class, in essence, calibrating the classical richness class designations. The median  $B_{gc}$  value of ARC 1 clusters in our sample is very close to  $1000 \text{ Mpc}^{1.8}$ . Hence, we propose to use  $1000 \text{ Mpc}^{1.8}$  as the fiducial  $B_{gc}$  value for the average ARC 1 counts.

Abell (1958) and ACO used a non-linear relationship between the Abell counts and the richness class with the higher ARC having disproportionately higher counts, presumably to account for the few apparently very high  $N_A$  clusters. However, §5.2 demonstrates that the very high  $N_A$  clusters are probably much less rich. If we scale the  $B_{gc}$  values corresponding to each ARC counts using the fiducial of  $1000 \text{ Mpc}^{1.8}$  as ARC 1, we see that there is a significant mismatch at  $\text{ARC} \geq 3$ , as illustrated by the dotted line in Figure 4, with ARC 5 being equivalent to  $B_{gc} \sim 7000$ . Yee et al. (1999) also found that none of the 16 clusters from the CNOC1 survey, which contains the most X-ray luminous clusters from the EMSS survey (see Gioia & Luppino 1994), have  $B_{gc}$  larger than  $\sim 2500 \text{ Mpc}^{-1.8}$ . Hence, there appears to be no known clusters that approach the original definition of ARC 5. In view of this, we propose a linear richness scale

where adjacent richness classes change by the same increment of  $400 \text{ Mpc}^{1.8}$  in  $B_{gc}$ . This scale would cover most of the range of known cluster richness (including very rich, X-ray luminous, higher redshift clusters, such as those in the CNOC1 sample), with the first 3 classes (0, 1, and 2) matching the original ARC definition reasonably well. This revised classification definition is shown graphically in Figure 4. For  $H_0 = 50 \text{ km s}^{-1} \text{ Mpc}^{-1}$ , the calibration for ARC 0 to 5 is then:  $600 \pm 200$ ,  $1000 \pm 200$ ,  $1400 \pm 200$ ,  $1800 \pm 200$ ,  $2200 \pm 200$ , and  $> 2400 \text{ Mpc}^{1.8}$ , respectively.

We note that this calibration is substantially different from those provided by Prestage & Peacock (1988) based on a very small number of 4C radio galaxies situated in Abell clusters. Their calibration of ARC 0 and 1 having  $B_{gc}$  of  $\sim 380$  and  $850 \text{ Mpc}^{1.8}$  is about 1/3 to 1/2 of an Abell class too high. Hence, previous descriptions of the Abell class equivalence for the environments of radio galaxies and quasars (e.g., YG87) need to be revised correspondingly downward.

#### 5.4. The Correlation Between Velocity Dispersion and Richness

So far we have shown that a richness parameter such as  $B_{gc}$ , which uses photometric data and normalized by the LF and spatial distribution of galaxies, produces a robust measurement of the richness of a cluster. One would then expect that such a robust parameter will provide a better description of the clusters, and hence produce more meaningful correlations with other cluster properties.

We will show, as a demonstration of the improvement expected, an example of such a correlation. One fundamental cluster property is the mass of a cluster, which can be estimated by the velocity dispersion ( $\sigma$ ). In Figure 6 we plot the correlation of  $\sigma$  versus  $B_{gc}$ . The velocity dispersion measurements are taken from the compilation of Struble & Rood (1991a), and Fadda et al. (1996). We include only those clusters with 10 or more velocity measurements. There is a clear correlation between  $\sigma$  and  $B_{gc}$ , and the correlation is much tighter than using  $N_A$  as the variable for richness which is shown in Figure 7. Girardi et al. (1993) showed a similar improvement in the correlation between velocity dispersion and richness when Bahcall’s (1981)  $N_{0.5}$  parameter is used instead of the Abell counts. This improved correlation lends support that  $B_{gc}$  is a more robust richness measurement.

The  $\sigma$ - $B_{gc}$  correlation derived from the CNOC1 cluster redshift survey (Yee et al. 1999) provides an even tighter correlation between the two quantities. This is almost certainly due to the fact that the velocity dispersion measurements from CNOC1 are derived from a homogeneous set of velocity data with a large number of velocities for each cluster. We note that the  $\sigma$ - $B_{gc}$  relationships derived from the two different samples (this work and CNOC1) are identical within the uncertainty. The  $\sigma$ - $B_{gc}$  relationship from CNOC1 is plotted as a dotted line in Figure 6. Given the different photometric systems used (Kron-Cousin  $R$  vs Gunn  $r$ ), the different redshift range of the sample, and the different instrumentations used for these two samples, this again points to the robustness of the  $B_{gc}$  measurements as a richness estimator.

## 6. Summary

We have used a sample of 47 Abell clusters with photometric catalogs from CCD images to test the robustness of  $B_{gc}$  as a parameter for measuring the richness of galaxy clusters. We first tested the effect of the choice of galaxy LF, which is used to normalize the excess galaxy counts. Using three LFs derived from different sources, including both cluster and field galaxies, we found that as long as we adjust the density normalization constant of the LF so that it reproduces the background counts used to derive the excess counts, different choices of the LF produce variations in  $B_{gc}$  of approximately 10%. Furthermore, the parameters for the LF can be substantially incorrect (e.g., with  $M^*$  being off by 0.5 mag), errors in  $B_{gc}$  can also be minimized by renormalizing the LF to fit the background counts.

We also found that if a correct LF is used, counting to different absolute magnitude limits produces systematic variations of only a few percent. However, to minimize uncertainties introduced by LF discrepancy and photometry errors, the results are most reliable when the counting is done to about 1 to 2 mag past  $M^*$ .

Similarly, the canonical  $\gamma = 1.8$  for the spatial correlation function of field galaxies provides reasonably stable  $B_{gc}$  values as one varies the radius of the counting aperture. Altering the counting radius from 0.25 to 1.5 Mpc produces systematic changes in  $B_{gc}$  of less than 10%.

We have compared our  $B_{gc}$  richness parameters with the Abell Richness Class and the Abell Count Number ( $N_A$ ). Limiting the sample to either  $\text{ARC} \leq 2$  or  $z \lesssim 0.1$ , we found a good correlation between  $N_A$  and  $B_{gc}$ . However, clusters designated as  $\text{ARC} \geq 3$  appear often to have their richness over estimated, sometimes by as much as a factor of 3. Since most of the  $\text{ARC} \geq 3$  clusters are at  $z > 0.1$ , this suggests that ARC classifications for clusters with  $z \gtrsim 0.1$  is not a good indicator of their true richness. We suggest a revised richness classification which is based on a linear scale in  $B_{gc}$ . Finally, we demonstrate the improvement in the correlation between richness and velocity dispersion when a robust richness parameter, like  $B_{gc}$ , is used.

We wish to thank KPNO for the generous allotment of telescope time and assistance in carrying out the Low-redshift Cluster Optical Survey (LOCOS). HY acknowledges NSERC for financial support in the form of an operating grant. OLC was supported in part by an overseas scholarship by CONACyT-México and INAOE. OLC also acknowledges financial support from the Department of Astronomy and the School of Graduate Studies of the University of Toronto, NSERC through HY’s operating grant, and CONACyT-México through a “Catedra de Repatriación” and a “Proyecto de Investigación Inicial.”

## REFERENCES

- Abell, G. 1958, *ApJS*, 3, 211
- Abell, G., Corwin, H.G., & Olowin, R.P. 1989, *ApJS*, 70, 1 (ACO)
- Anderson, V. & Owen, F. 1994, *AJ*, 108, 361
- Bahcall, N. 1981, *ApJ*, 247, 787
- Carlberg, R.G., Yee, H.K.C., & Ellingson, E. 1997, *ApJ*, 478, 462
- Carlberg, R.G., Yee, H.K.C., Ellingson, E., Abraham, R.G., Gravel, P., Morris, S.L., & Pritchet, C.J. 1996, *ApJ*, 462, 32
- Davis, M. & Peebles, P.J.E. 1983, *ApJ*, 294, 70
- De Robertis, M.M., Yee, H.K.C., & Hayhoe, K. 1998, *ApJ*, 496, 93
- Dickinson, M.E. 1997, in *The Hubble Space Telescope and the High Redshift Universe*, eds N. Tanvir et al., (World Scientific : Singapore), page 207
- Dressler, A. 1978, *ApJ*, 226, 55
- Driver, S.P., Phillipps, S., Davies, J.I., Morgan, I., & Disney, M.J. 1994, *MNRAS*, 266, 155.
- Ellingson, E., Yee, H.K.C., & Green, R.F. 1991, *ApJ*, 371, 49
- Fadda, D., Girardi, M., Giuricin, G., Mardirossian, F., & Mezzetti, M. 1996, *ApJ*, 473, 670
- Gioia, I.M. & Luppino, G.A. 1994, *ApJS*, 94, 583
- Girardi, M., Biviano, A., Giuricin, G., Mardirossian, F., & Mezzetti, M. 1993, *ApJ*, 404, 38
- Jones, C. & Forman W. 1998, preprint
- King, C., & Ellis, R.S. 1984, *ApJ*, 288, 456 (KE)
- Landolt, A. 1992, *AJ*, 104, 340
- Lilje, P.B. & Efsthathiou, G. 1988, *MNRAS*, 231, 635
- Lin, H., Yee, H.K.C., Carlberg, R.G., Morris, S., Sawicki, M., Patton, D., Wirth, G., & Shepherd, C.W. 1999, *ApJ*, in press
- Longair, M.S., & Seldner, M. 1979, *MNRAS*, 189, 433
- López-Cruz, O. 1997, Ph. D. thesis, University of Toronto (LC97)
- López-Cruz, O., & Yee, H.K.C. 1999, to be submitted to *ApJ* (LCY)
- López-Cruz, O., Yee, H.K.C., Brown, J.P., Jones, C., & Forman, W. 1996, *ApJ*, 476, L97
- Metcalfe, N., Shanks, T., Fong, R. & Jones, L. R. 1991, *MNRAS*, 249, 498
- Peebles, P.J.E. 1993, *Principles of Physical Cosmology*, (Princeton University Press : Princeton), page 471
- Prestage, R.M. & Peacock, J.A. 1988, *MNRAS*, 230, 131



- Smith, E.P., O’Dea, C.D., & Baum, S. 1995, *ApJ*, 441, 113
- Schechter, P.L. 1976, *ApJ*, 203, 297
- Southerland, W. 1988, *MNRAS*, 234, 159
- Struble, M.F. & Rood, H.J. 1991a, *ApJS*, 77, 363
- Struble, M.F. & Rood, H.J. 1991b, *ApJ*, 374, 398
- Tyson, J.A. & Fischer, P. 1996, *ApJ*, 446, L55
- Wurtz, R., Stocke, J.T., Ellingson, E., Yee, H.K.C. 1997, *ApJ*,
- Yates, M.G., Miller, L., & Peacock, J.A. 1989, *MNRAS*, 240, 129
- Yee, H.K.C. 1991, *PASP*, 103, 396
- Yee, H.K.C., Ellingson, E., Morris, S., & Carlberg, R.G. 1999, preprint to be submitted to *ApJ*
- Yee, H.K.C., & Green, R.F. 1984, *ApJ*, 280, 79
- Yee, H.K.C., & Green, R.F. 1987, *ApJ*, 319, 28 (YG87)
- Yee, H.K.C., Green, R.F., & Stockman, H.S. 1986, *ApJS*, 62, 681
- Yee, H.K.C. et al. 1997, in the proceedings of the IAU Joint Discussion 11: Redshift Surveys in the 21st Century, ed. A. Fairall, in press (astro-ph/9710356)

Fig. 1.— Background galaxy counts in Cousin  $R$  from 9 KPNO 0.9m fields. The dashed, dotted, and solid lines represent the count models created using the LCY LF, KE LF, and CNOC2 LF, respectively.

Fig. 2.— Comparison of  $B_{gc}$  values computed using counting magnitude limits of  $-20.0$  and  $-21.0$ . The former cut-off is equivalent to  $M^* - 1.7$ . The dotted line is not a fit, but a line of slope unity.

Fig. 3.— Comparison of  $B_{gc}$  values computed using counting radii of  $0.5$  Mpc and  $1.0$  Mpc. The dotted line is not a fit, but a line of slope unity.

Fig. 4.— The correlation between Abell Richness Class and the  $B_{gc}$  parameter. The median  $B_{gc}$  value for each ARC is shown as an asterix. The dot-dashed line indicates the expected  $B_{gc}$  values for each ARC which describes the relative median richness of ARC 1 and 2 well, but fails significantly for richer classes. The six bars connected by the dashed line illustrates a linear richness classification which matches the real richness of the various ARC reasonably well.

Fig. 5.— The correlation between Abell count number and the  $B_{gc}$  parameter. Solid symbols represent cluster with  $z < 0.09$ ; while open symbols mark clusters with  $z > 0.09$ . The solid star symbols are Abell clusters at  $\sim 0.2$  from the CNOC1 survey. The dashed line shows the best fitting line for the  $z < 0.09$  subsample force-fitted through the origin, while the dotted line is the best linear fit for the  $z > 0.09$  subsample.

Fig. 6.— The correlation between velocity dispersion and cluster richness as parametrized by  $B_{gc}$ . The dashed line is the best linear fit; while the dotted line shows the relationship derived from 15 CNOC1 clusters (Yee et al. 1999).

Fig. 7.— The much poorer correlation between velocity dispersion and cluster richness as parametrized by the Abell count number ( $N_A$ ).

Table 1. Abell Clusters

Cluster	$z$	ARC	$B_{gc}$	$\pm$
A21	0.0946	1	1509	241
A84	0.1030	1	1000	204
A85	0.0518	1	757	174
A98	0.1043	3	1921	268
A154	0.0638	1	1393	230
A168	0.0452	2	973	192
A399	0.0715	1	1449	235
A401	0.0748	2	2242	286
A407	0.0472	0	1368	225
A415	0.0788	1	534	159
A514	0.0731	1	946	196
A629	0.1380	1	1205	224
A646	0.1303	0	858	196
A665	0.1816	5	2186	290
A671	0.0491	0	1266	217
A690	0.0788	1	701	175
A957	0.0437	1	1075	201
A1213	0.0469	1	931	189
A1291	0.0530	1	1122	207
A1413	0.1427	3	1686	257
A1569	0.0784	0	768	181
A1650	0.0845	2	1861	263
A1656	0.0232	2	1242	282
A1775	0.0700	2	1018	202
A1795	0.0621	2	1430	233
A1913	0.0530	1	954	192
A1983	0.0430	1	974	192
A2029	0.0768	2	1736	255
A2244	0.0997	2	1698	254
A2255	0.0800	2	2296	289
A2256	0.0601	2	2174	281
A2271	0.0568	0	645	164
A2328	0.1470	2	1941	273
A2356	0.1161	2	944	201
A2384	0.0943	1	1575	245
A2399	0.0587	1	906	190

Table 1—Continued

Cluster	$z$	ARC	$B_{gc}$	$\pm$
A2410	0.0806	1	699	175
A2415	0.0597	0	902	190
A2420	0.0838	2	1230	220
A2440	0.0904	0	1053	207
A2554	0.1108	3	1218	222
A2556	0.0865	0	828	187
A2593	0.0421	0	1211	212
A2597	0.0825	0	665	172
A2626	0.0573	0	945	193
A2657	0.0414	1	740	170
A2670	0.0761	3	1771	257

Table 2. Luminosity Functions

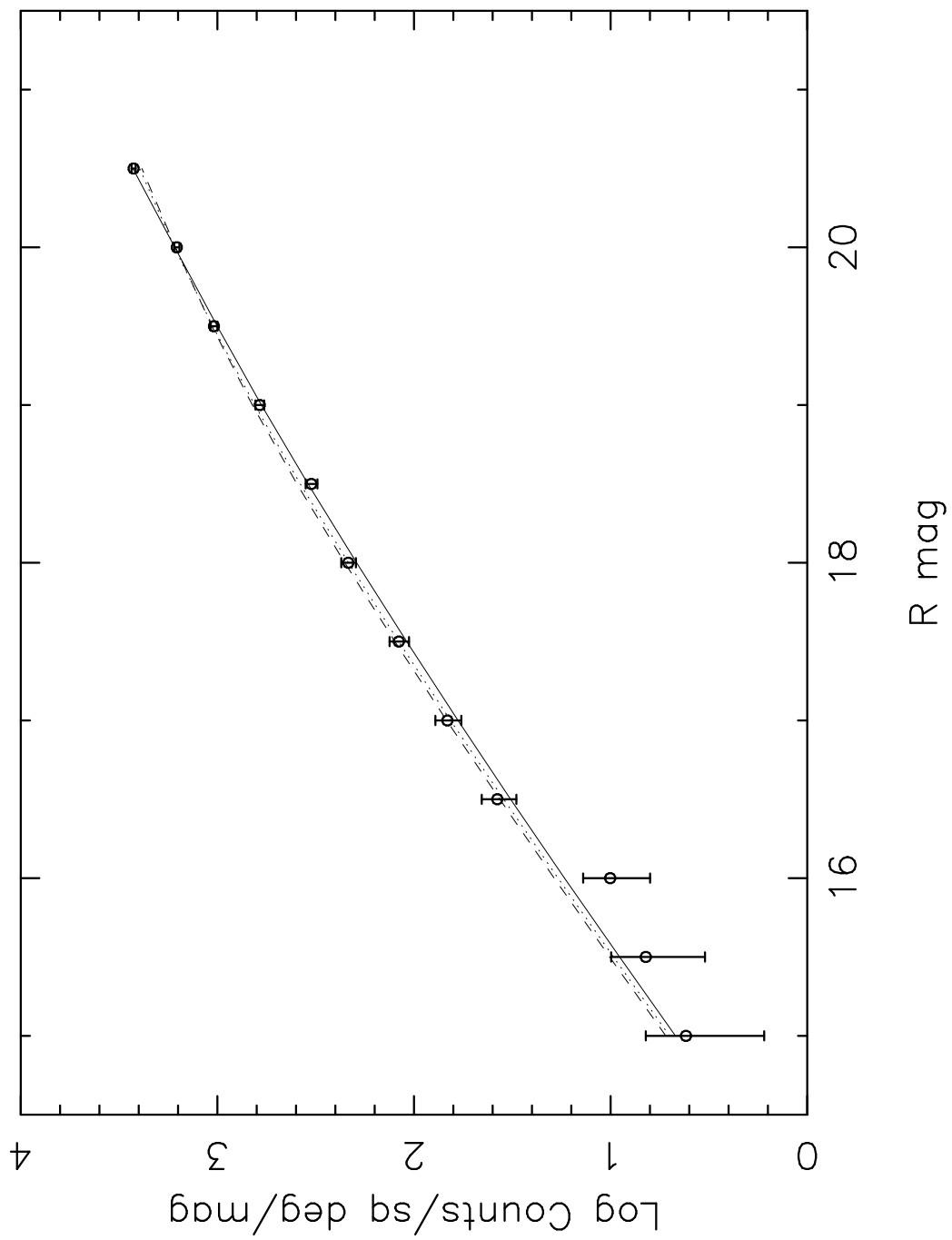
LF	galaxy type	$\phi'$	$\phi^*$	$\alpha$	$M^*$	$Q$	$P$
LCY	cluster	0.00226	1.0	−1.00	−22.20	1.4	0.0
KE	E/S0	0.000346	1.79	−1.00	−22.45	1.4	0.0
	Sab	0.000346	1.87	−1.00	−22.14	1.4	0.0
	Sbc	0.000346	1.87	−1.00	−21.81	1.4	0.0
	Scd/Sdm	0.000346	3.24	−1.00	−21.29	0.7	0.0
CNOC2	early	0.92	0.00212	0.09	−21.52	1.94	−2.02
	intermediate	0.92	0.00111	−0.69	−21.84	0.62	0.59
	late	0.92	0.00053	−1.45	−21.44	0.88	2.68

Table 3. Fractional Change to mean  $B_{gc}$  Adjusting  $M^*$

Sampling Limit	LF Renormalization	$\Delta M^*$ :	−0.50	−0.25	0.00	+0.25	+0.50
−20	yes		1.24	1.11	1.00	0.91	0.84
−20	no		0.80	0.89	1.00	1.14	1.32
−22	yes		0.90	0.95	1.03	1.18	1.42
−22	no		0.58	0.76	1.03	1.47	2.24

Table 4. Fractional Change to mean  $B_{gc}$  Adjusting  $\alpha$

Sampling Limit	LF Renormalization	$\Delta\alpha$ :	−0.30	−0.15	0.00	+0.15	+0.30
−20	yes		0.92	0.96	1.00	1.10	1.19
−20	no		0.73	0.86	1.00	1.14	1.29
−22	yes		1.39	1.19	1.03	0.95	0.87
−22	no		1.11	1.07	1.03	0.99	0.94



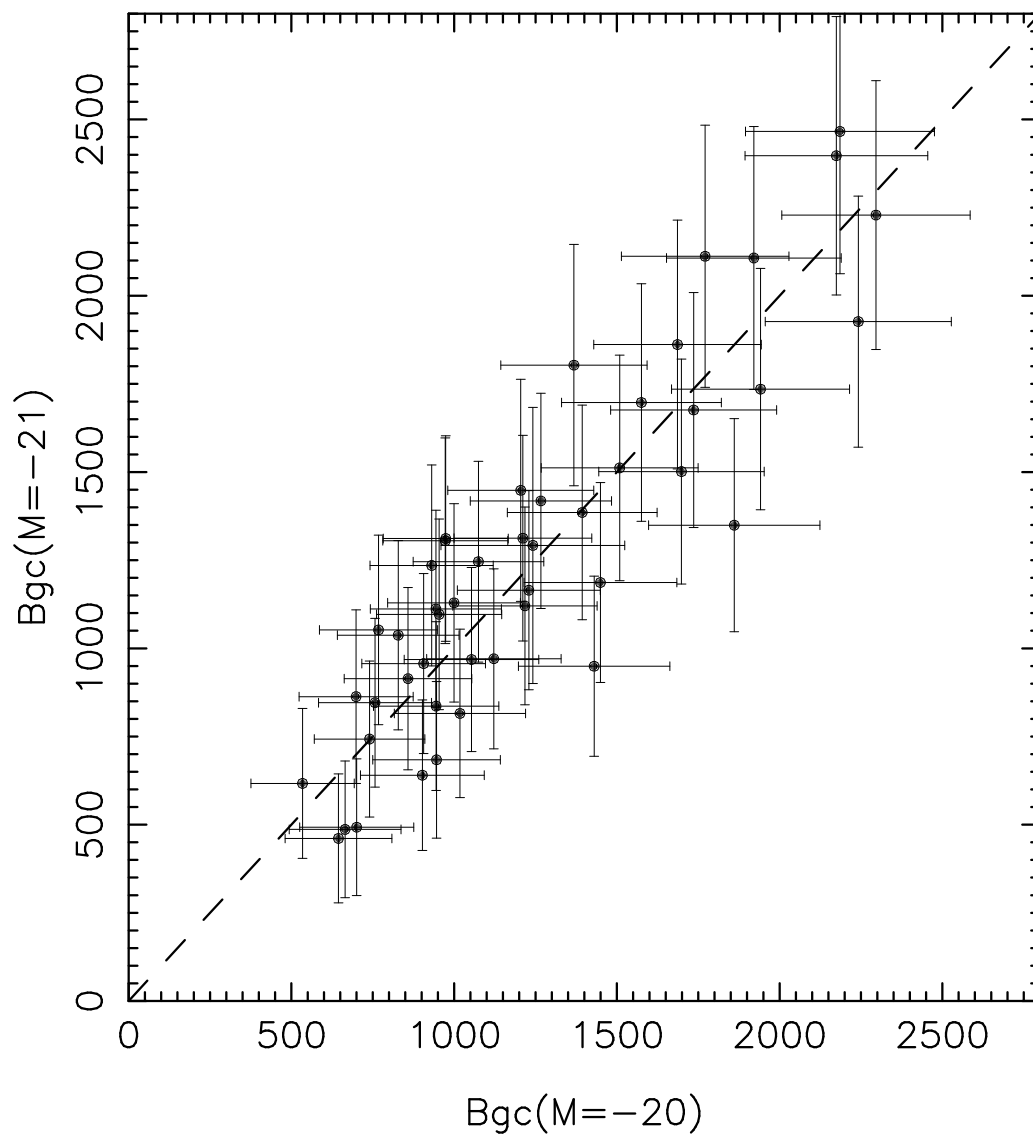


Fig. 2.—

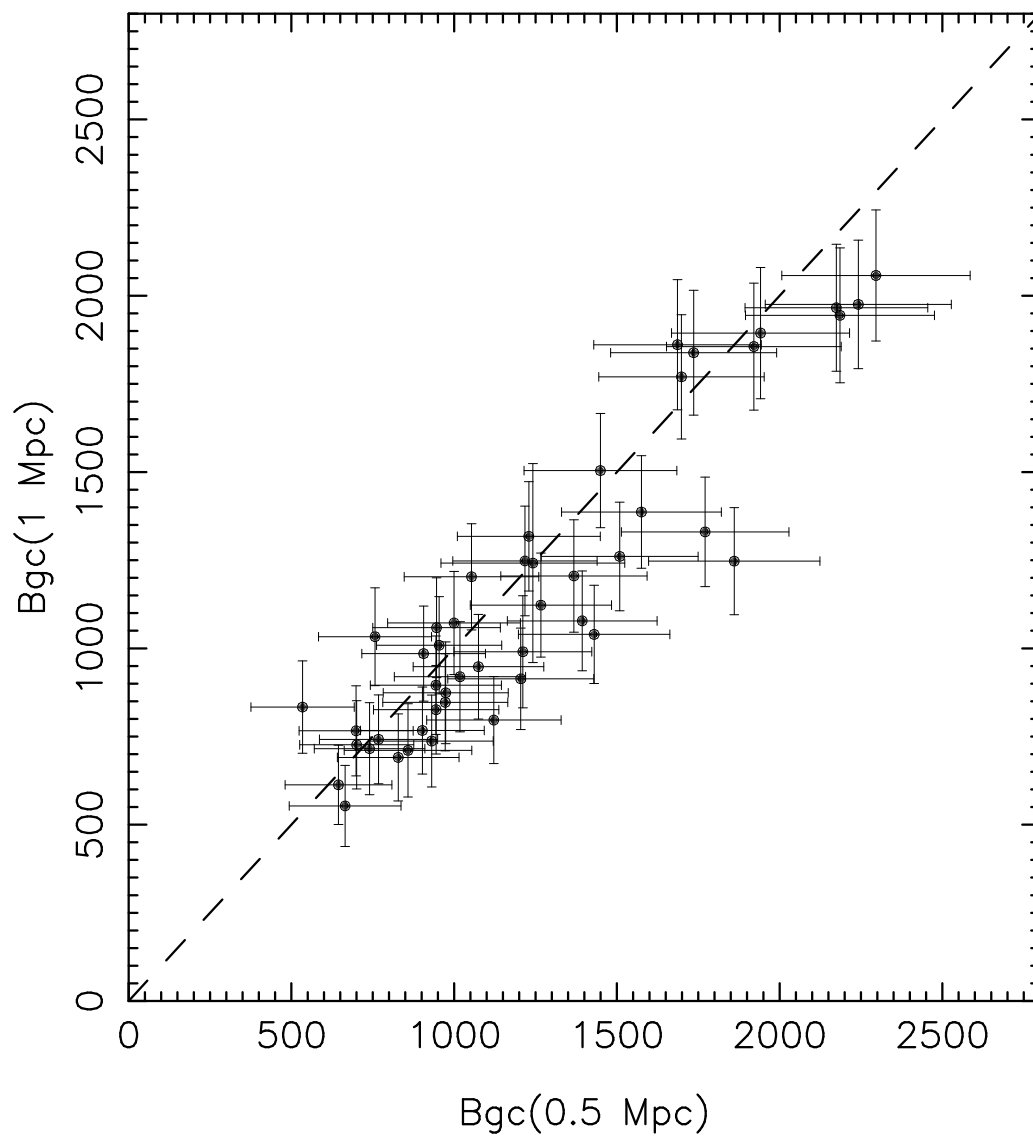


Fig. 3.—



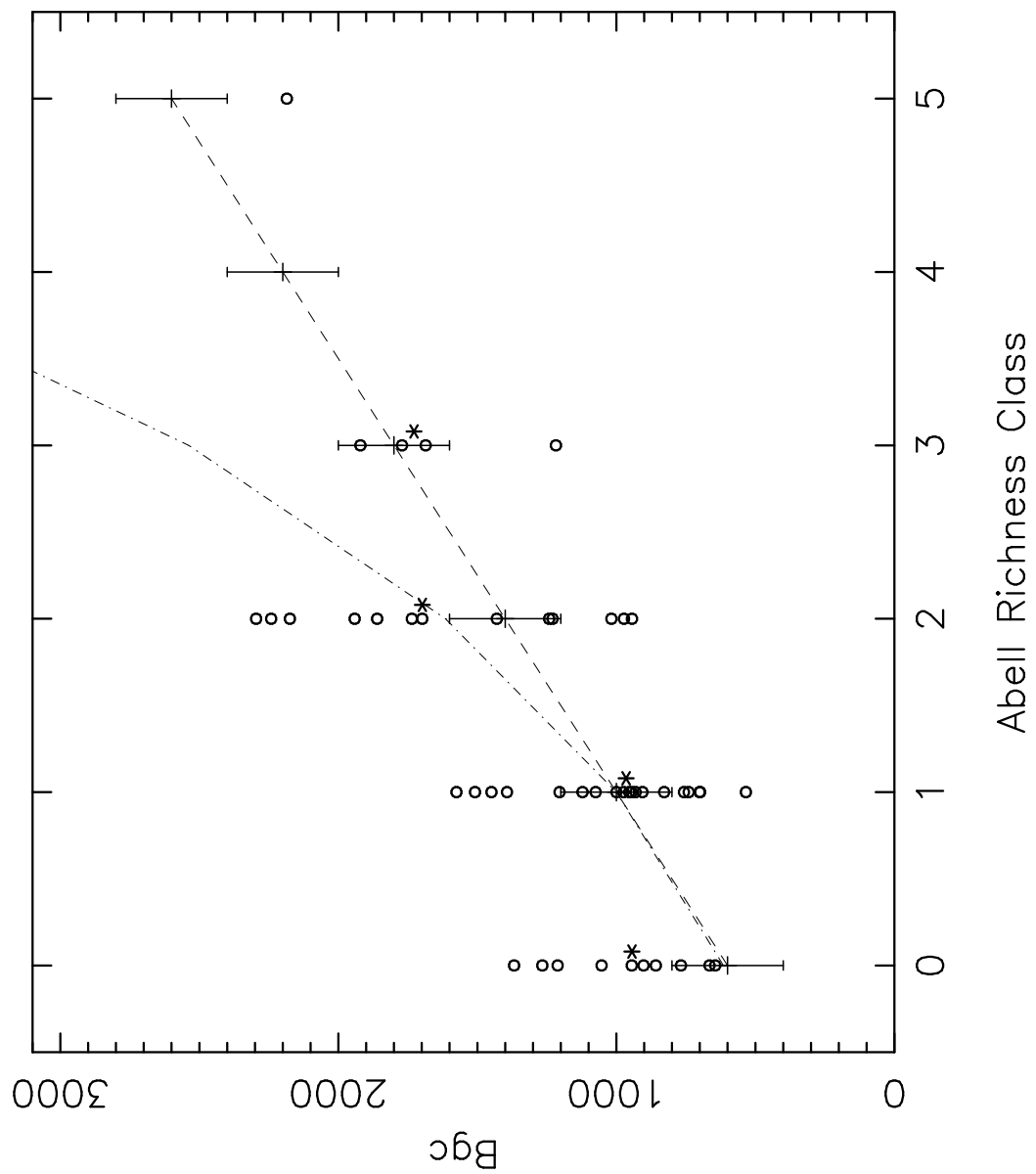


Fig. 4.—

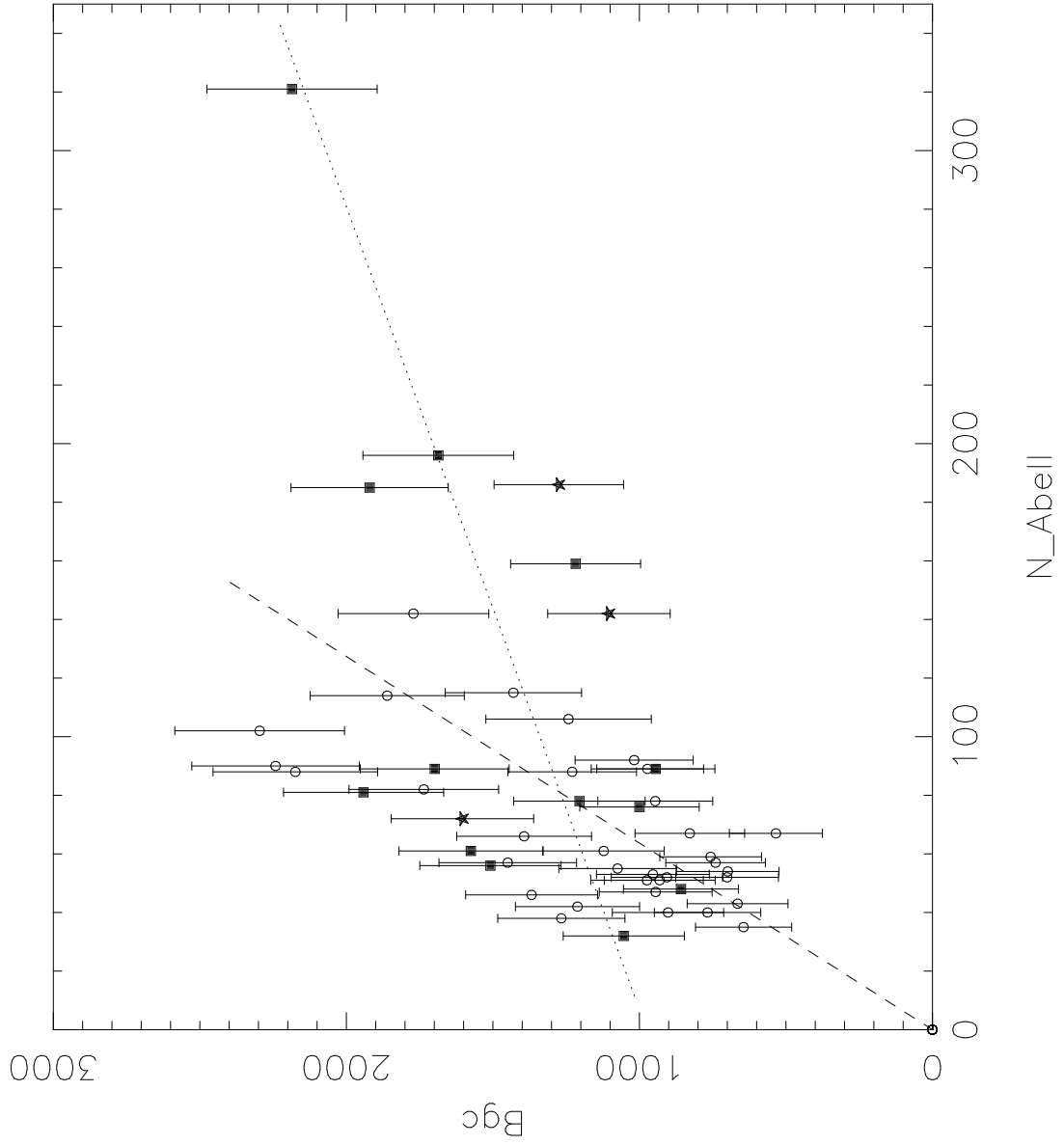


Fig. 5.—

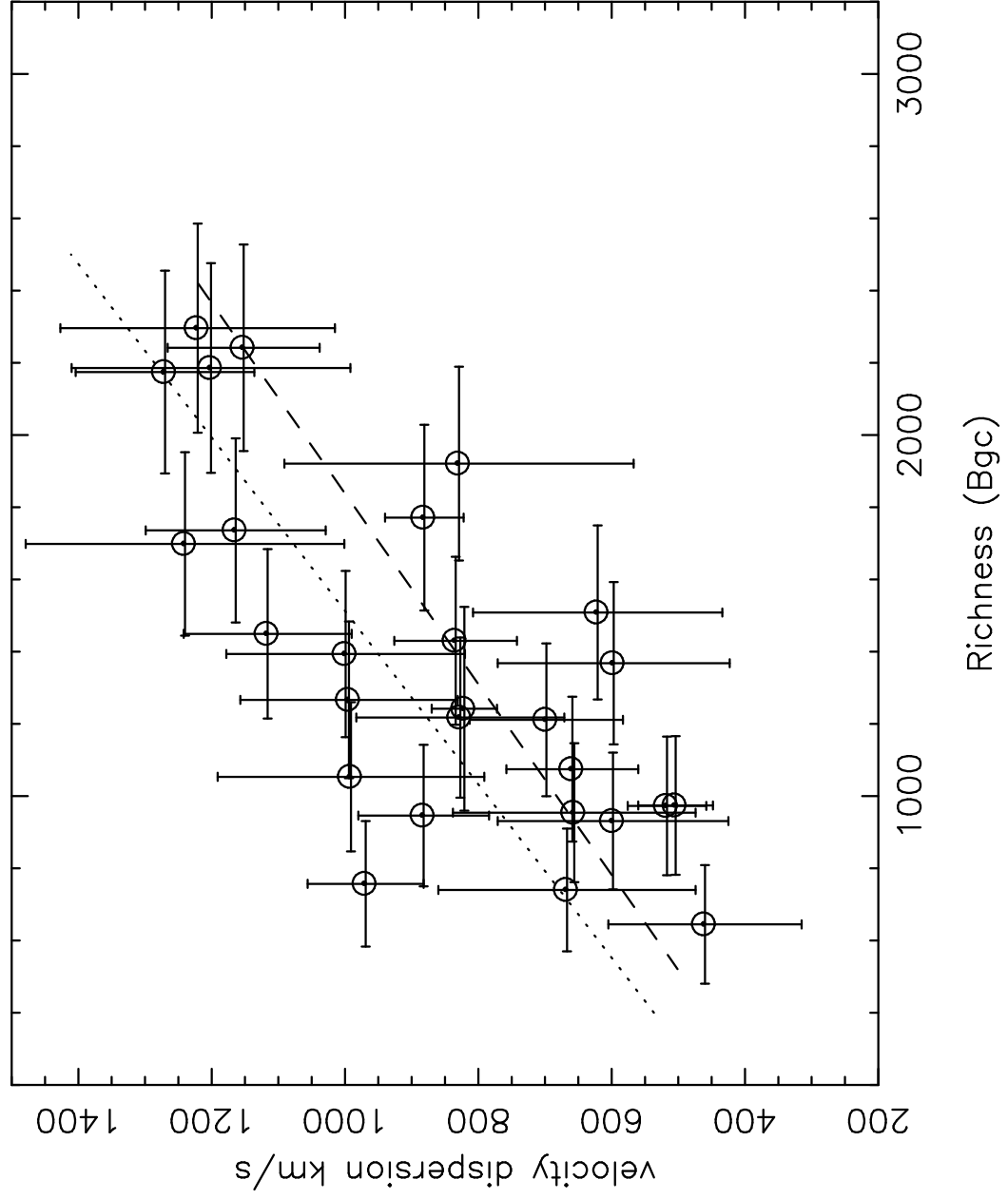


Fig. 6.—

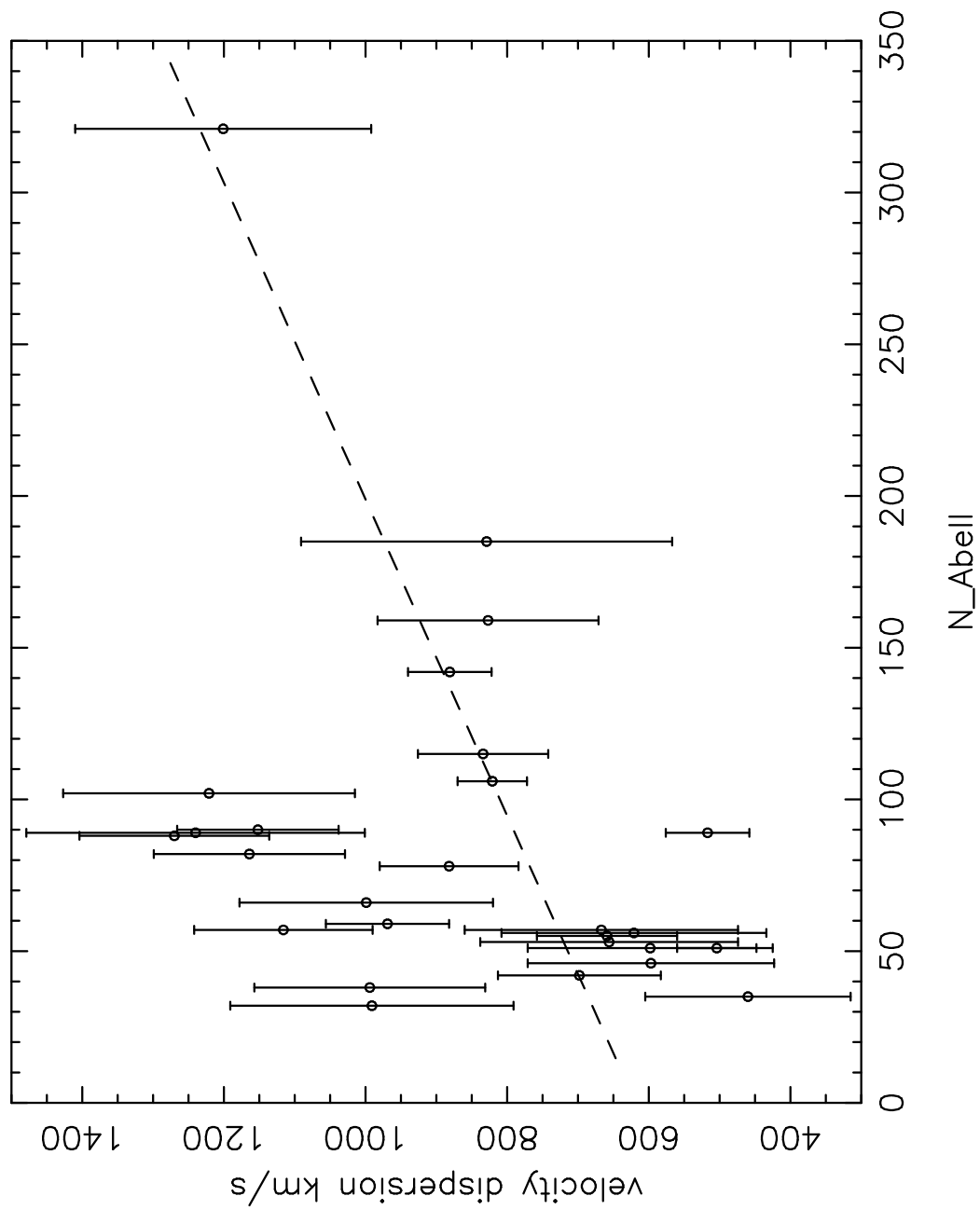


Fig. 7.—